國立交通大學
National Chiao Tung University

Aerodynamics of Sport Balls

王啟川, PhD
國立交通大學機械工程系教授
Fellow ASME, Fellow ASHRAE
Tel: 3-5712121 ext. 55105
E-mail:ccwang@mail.nctu.edu.tw

Outline

- Background
- Basic Fluid Mechanics
- Non-spinning vs. spinning ball
- Baseball aerodynamics
- Golf ball areodynamics
- Tennis ball areodynamics
- Some preliminary observations for table tennis ball
- Summay

Background

- Ball can be made to deviate from its initial straight path, resulting in a curved flight path.
- It is particularly fascinating that not all the parameters that affect the flight of a ball are under human influence. Lateral deflection in flight (variously known as swing, swerve, or curve) is well recognized in cricket, baseball, golf, and tennis.

Figure 3. A Modern Day Golf Ball. Diameter = 4.27 cm, Mass = 0.046 kg, Typical $Re = 2 \times 10^5$.

Figure 4. Modern Day Soccer Ball. Diameter = 22.3 cm, Mass = 0.44 kg, Typical $Re = 3.9 \times 10^5$.

Figure 5. A Modern Day Volleyball. Diameter = 21 cm, Mass = 0.27 kg, Typical $Re = 2.8 \times 10^5$.

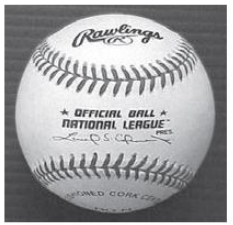

Figure 6. An Official (National League) Baseball. Diameter = 7.23 cm. Mass = 0.156 kg, Typical $Re = 1.5 \times 10^5$.

Basic Fluid Mechanics

- The Bernoulli Eq.

$p+1/2\rho u^2+\rho gh=C$

Where

p:static pressure

ρ: density

u: velocity

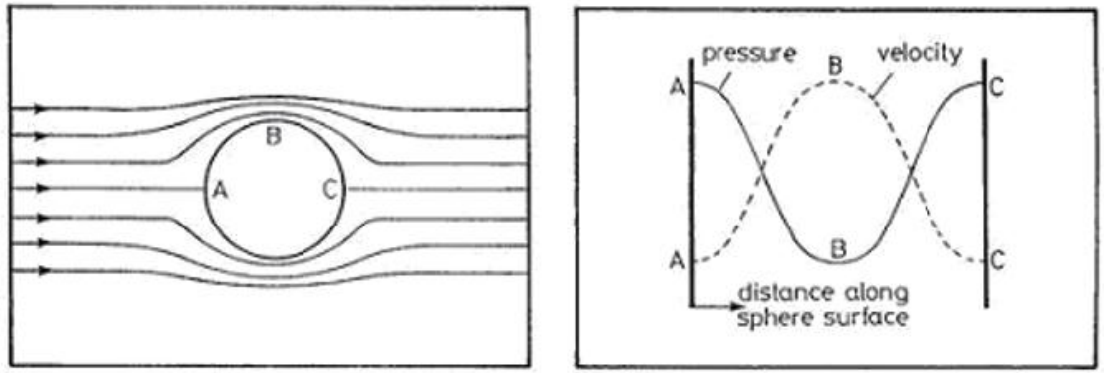

Figure 7. (a) Inviscid flow over a sphere. (b) Pressure and velocity distributions for inviscid flow over a sphere (Mehta & Wood 1980).

Applicable to

Invisid, Incompressible flow

Real Fluids..

- Sticky & Viscous
- At the surface, no-slip prevails
- Forming a boundary layer near the object
- It depends on the flow type – laminar or turbulent
- Adverse velocity gradient

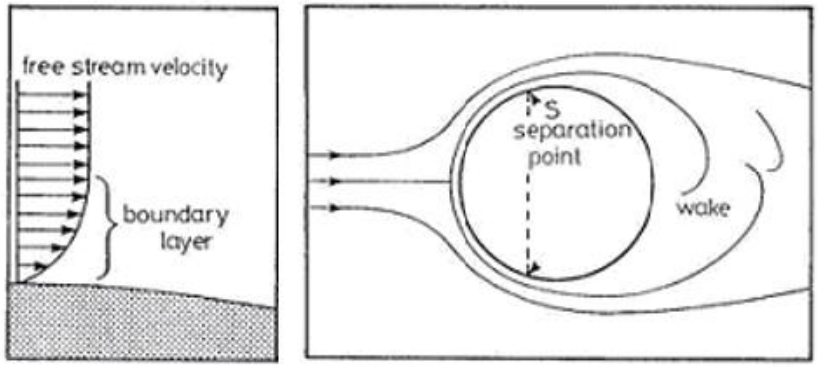

Figure 8. Boundary layer profile and development over a sphere for a viscous fluid (Mehta & Wood 1980).

More on velocity profile and separation

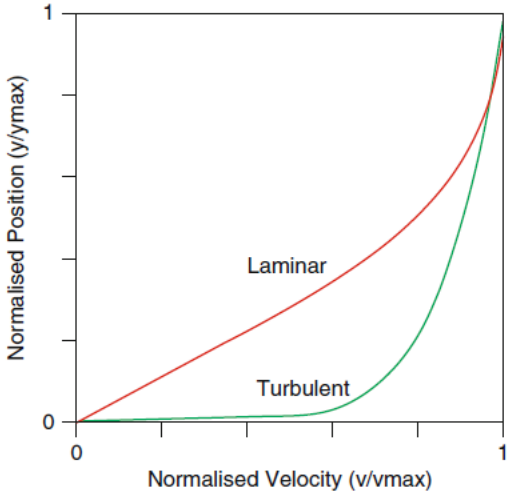

Fig. 1 Laminar and turbulent boundary layer velocity profiles [3]

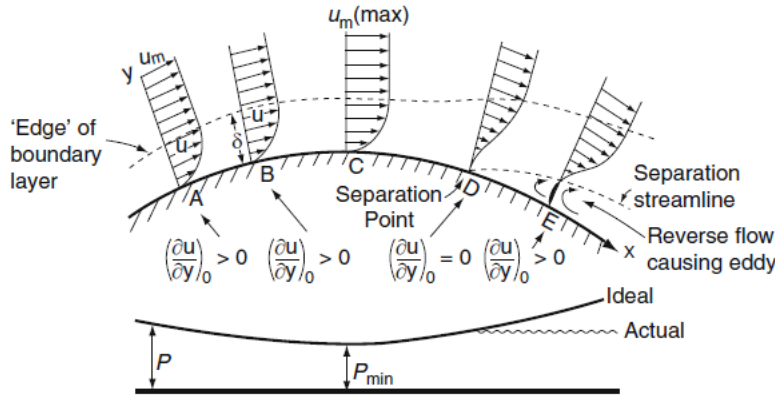

Fig. 2 Mechanism of boundary layer separation over a curved surface [3]

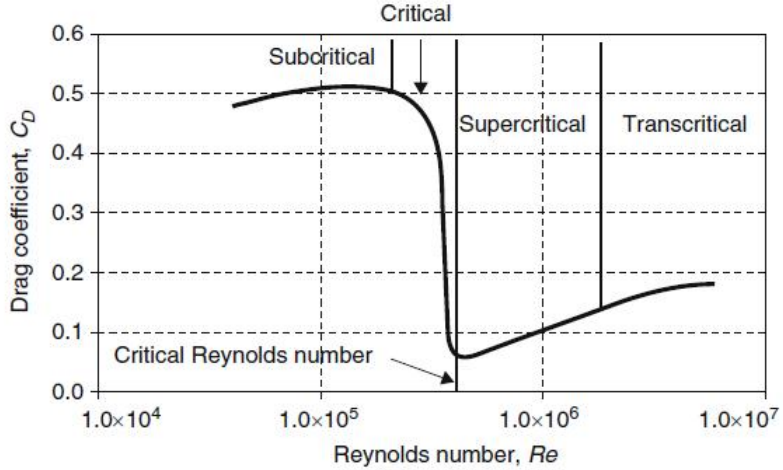

Fig. 3 C_D vs. Re for a smooth sphere, game-relevant Re [4]

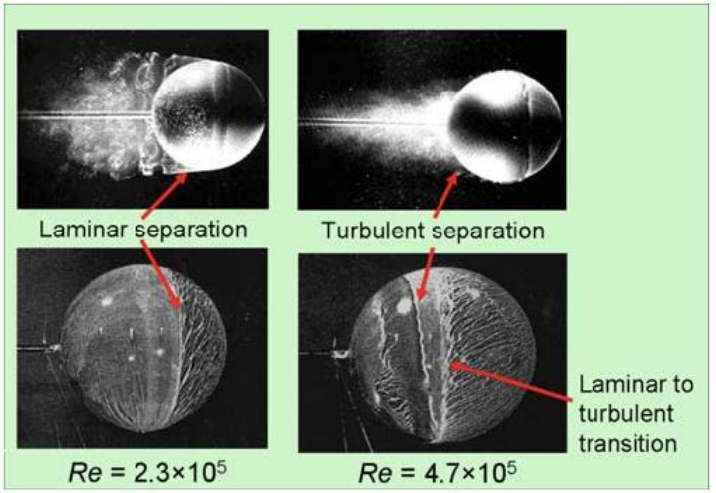

Fig. 4 Smoke flow (*top*) [5] and oil flow visualization (*bottom*) [6] for a smooth sphere, flow from right to left

The forces on a non-spinning flying object

- **Lift**, the upward acting force
- **Weight** (or gravity), the downward acting force
- **Thrust**, the forward acting force
- **Drag**, the rearward acting, or retarding, force.

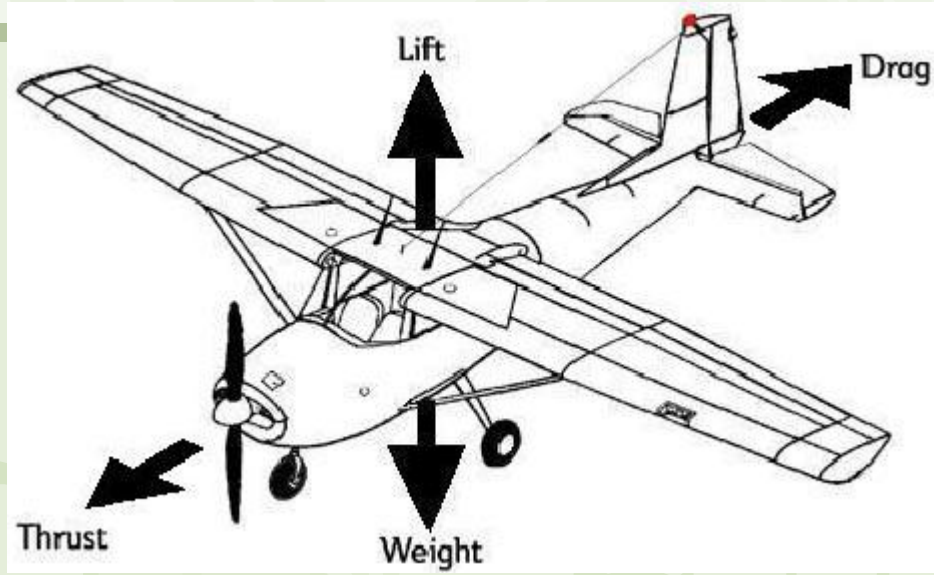

Coefficient of Lift $C_L = \frac{L}{\frac{1}{2}\rho V_\infty^2 A}$ Where, L=Lift, ρ=air density, V=velocity, and A= frontal area

Coefficient of Drag $C_D = \frac{D}{\frac{1}{2}\rho V_\infty^2 A}$ Where, D=Drag, ρ=air density, V=velocity, and A= frontal area

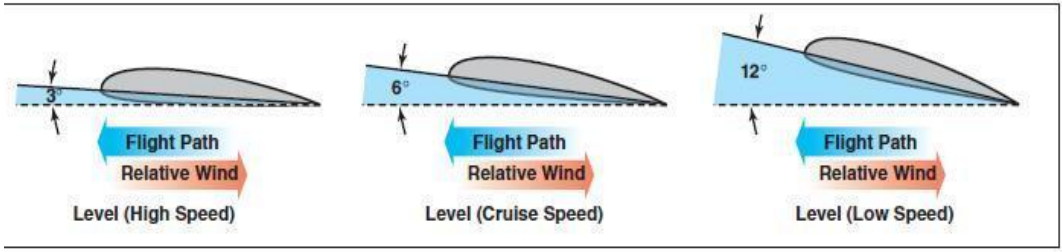

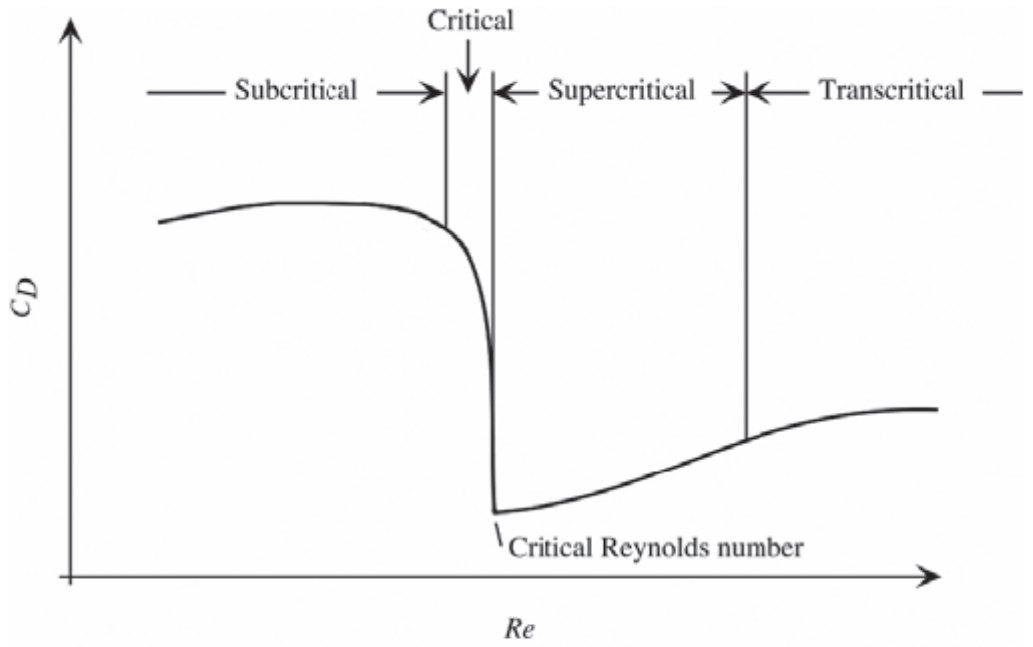

Figure 13. Flow regimes on a sphere (based on Achenbach 1972).

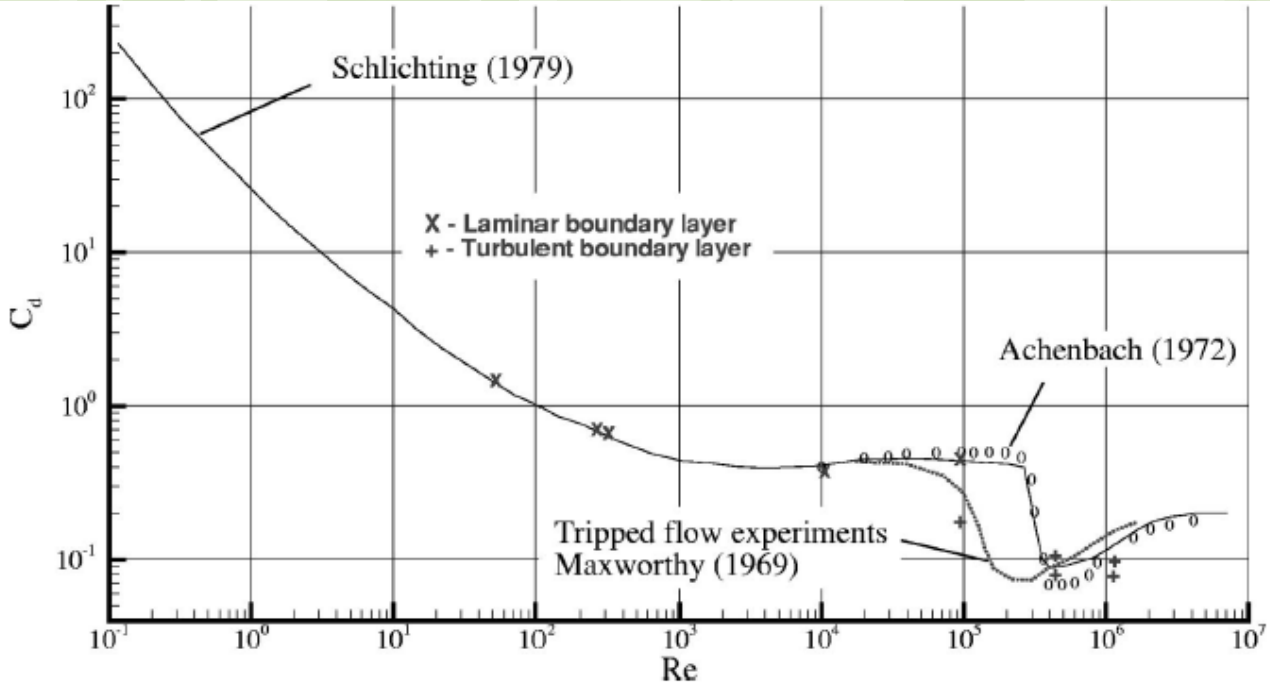

FIG. 1. Drag coefficient for uniform flow over a sphere as a function of the Reynolds number. Experimental data from Schlichting (1979), Achenbach (1972), and Maxworthy (1969).

PHYSICS OF FLUIDS
VOLUME 16, NUMBER 5,
2004, 1449-1466.

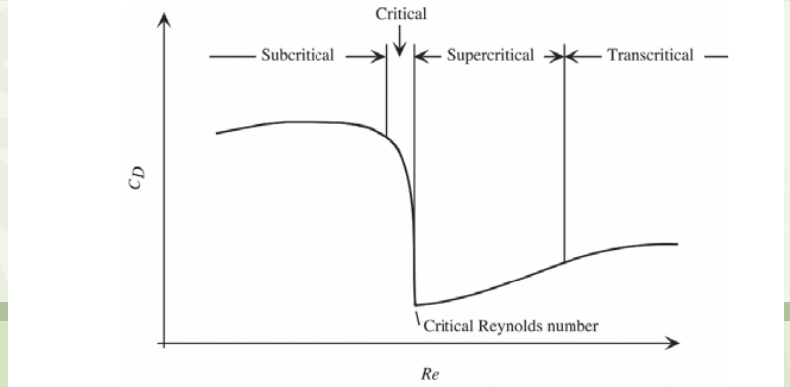

- In the laminar flow region, separation occurs at an angle around 80°, and C_d is nearly independent of Re.
- C_d drop quickly at the critical region.
  - The initial drop is due to separation pt. being moved to downstream (~95 °).
- The turbulent BL is able to withstand adverse pressure gradient, and the separation is delayed to 120°.
- In the supercritical region, transition occurs and the separation creeps upstream, resulting a rise of C_d.
- The limit is reached when the separation moves near to the stagnation point, C_d becomes nearly independent of Re since further increase of Re can not change the separation pt.
- In the region, C_d is mainly related to roughness.

Flow Past a non-spinning Sphere

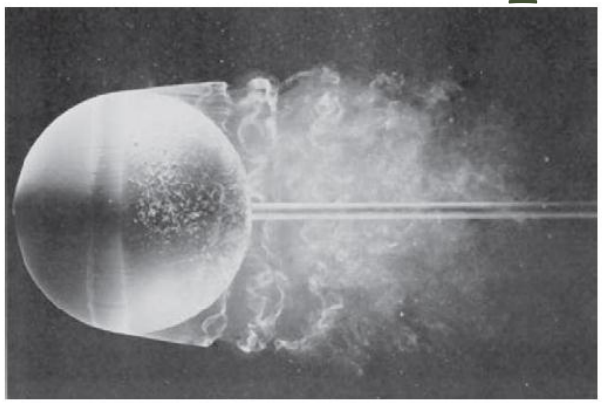

Figure 11. Laminar boundary layer separation on a smooth sphere; boundary layer separates near the sphere apex. Flow is from left to right and note that a wide wake implies high drag (from Van Dyke 1982, photograph by H. Werlé 1980, copyright ONERA, the French Aerospace Laboratory).

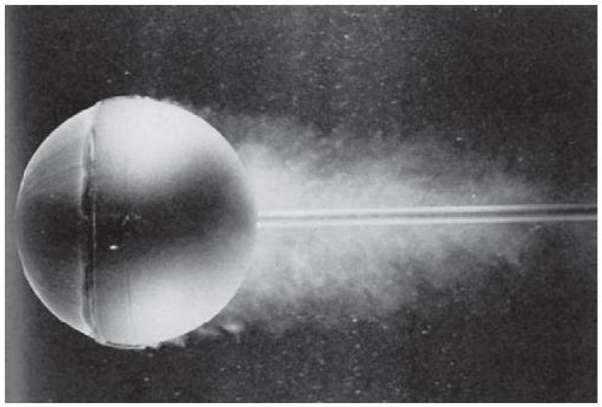

Figure 12. Turbulent boundary layer separation; boundary layer is tripped into a turbulent state by a thin wire attached to the front of the sphere and separation is delayed. Flow is from left to right and note the narrower wake compared to that in Fig. 11, implying lower drag (from Van Dyke 1982, photograph by H. Werlé 1980, copyright ONERA, the French Aerospace Laboratory).

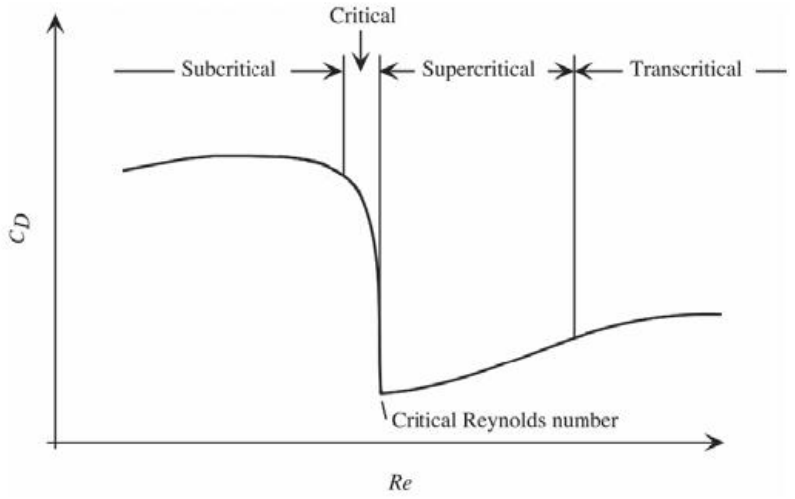

Figure 13. Flow regimes on a sphere (based on Achenbach 1972).

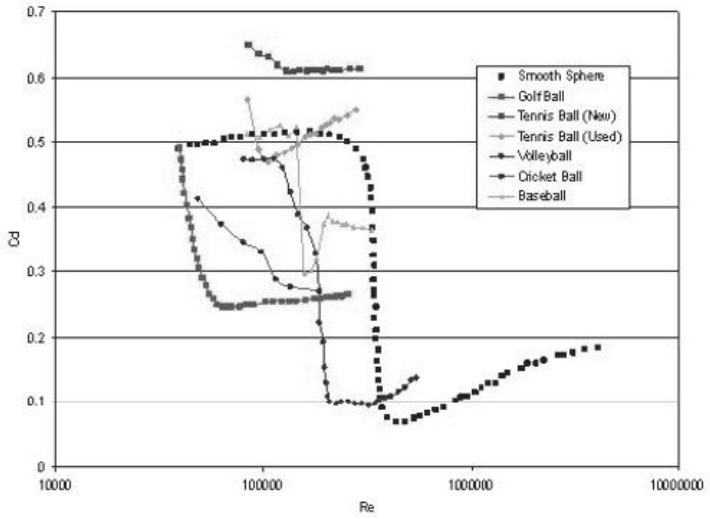

Figure 14. Drag coefficient versus Reynolds number for different nonspinning sports balls (Mehta & Pallis 2001a).

Non-spinning vs. Spinning Ball..

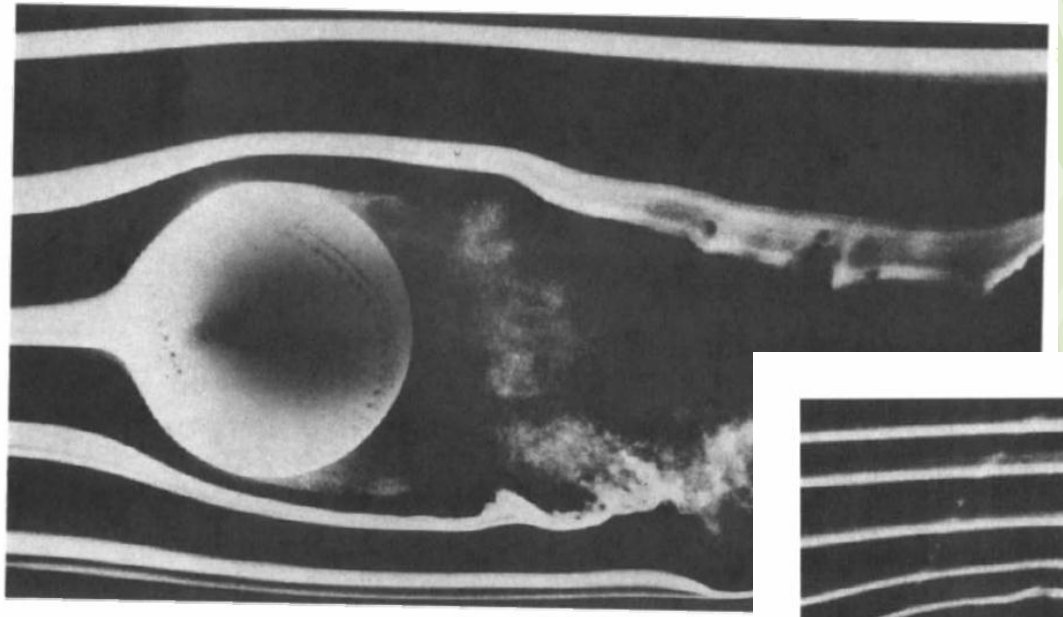

Figure 13 Smoke photograph of flow over a stationary (nonspinning) baseball. Flow is from left to right. Dame University (Brown 1971).

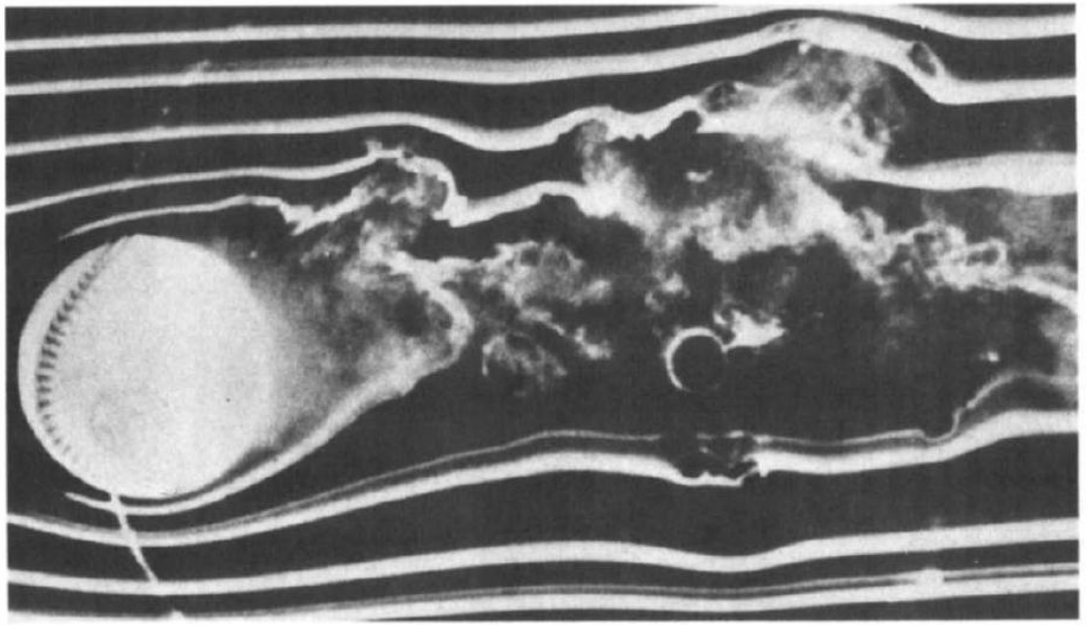

Figure 12 Smoke photograph of flow over a spinning baseball. Flow is from left to right, and the flowspeed is 21 m s^{-1}. The baseball is spinning in a counterclockwise direction at 15 rev s^{-1}. Photograph by F. N. M. Brown, Notre Dame University (Brown 1971).

Magnus Effect

- When a cylindrical body or a spherical spins and moves in one direction through a fluid, experiences a force perpendicular to the direction of its velocity.

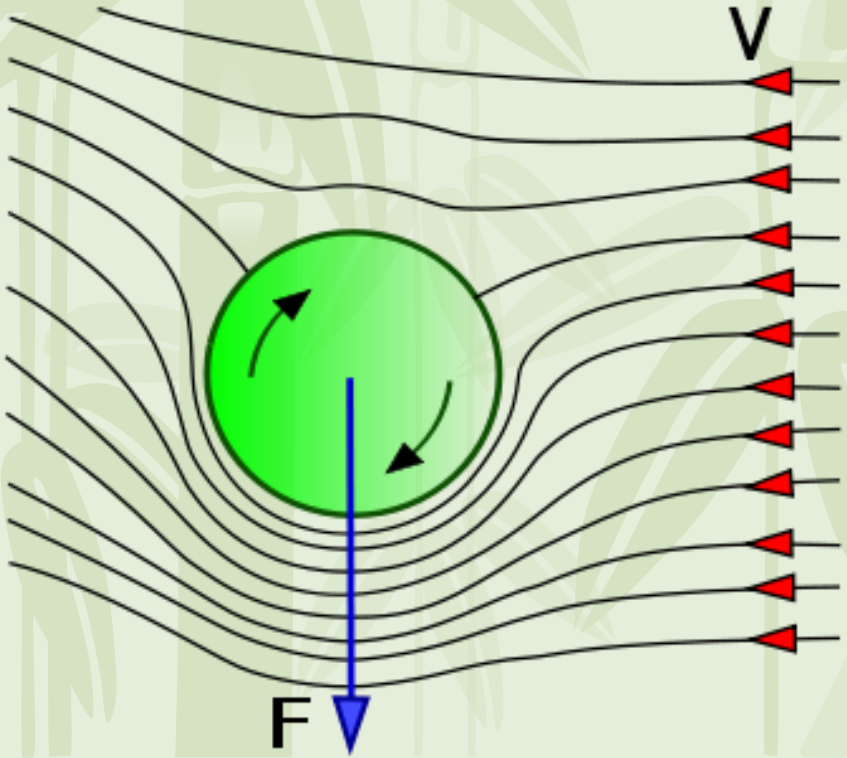

Heinrich Gustav Magnus (1802-1870)

Major interests of sports aerodynamics

- Drag force, or C_d
- Lift force, or C_L
- Effect of spinning, S (spinning factor)
- Effect of specific parameters (seam, seam orientation, geometry and the like.
- Trajectory path

- Approaches..
  - Experimental study (test on site)
  - Experimental study (with controlled equipments)
  - Experimental study (wind tunnel – normally with downsize ball)
  - Numerical study

Aerodynamics of Baseball

- Hour-glass like segments (2 segments)
- Made of white leather seamed together by 216 stitches.
- Baseball curve in flight is related to spin and asymmetric boundary-layer tripping due to seam position.

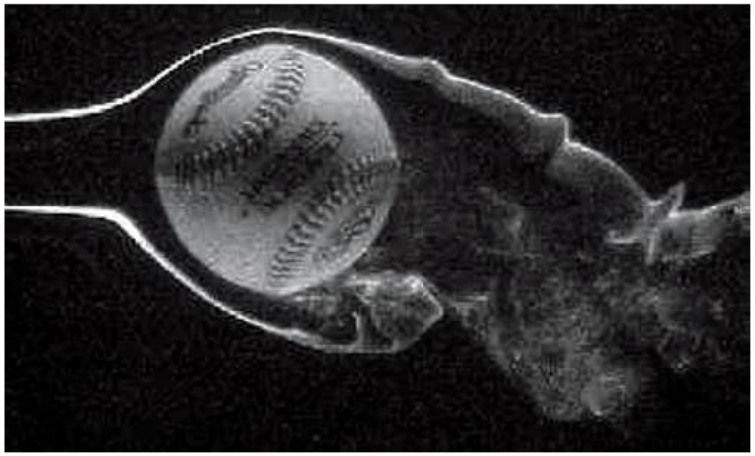

Figure 71. Flow visualization of a spinning baseball at $Re = 3400$; flow is from left to right and the ball is spinning in a clockwise direction at 0.5 revs/sec (Pallis and Mehta 2003).

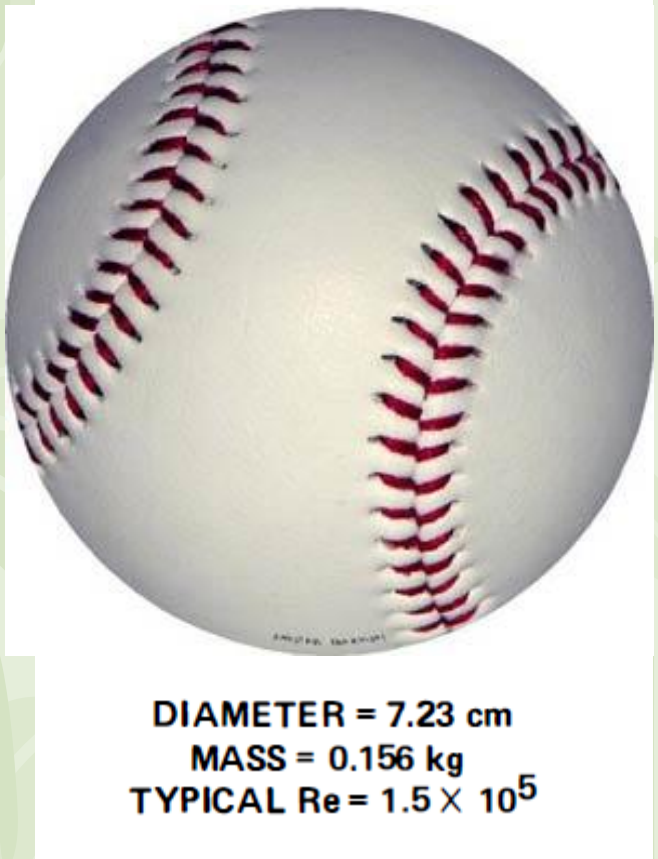

Example – A curve Ball

- Spinning with effect of drag/lift & gravity.
- Gravity effect moves object fast over time.
- The ball becomes more pronounced as it reaches home base
  - Normally a pitch drop ½ foot in the first half of the flight and another 2 feet in the second half.
  - In typical topspin ball, additional Magnus force is imposed on the ball which along with the gravity drops the ball further.
  - Round house curve ball – thrown with addition of twist of wrist.

Non-spinning Baseball

- It still shows asymmetric boundary layer due to presence of seam location. Seam acts like a roughness which play an essential role .

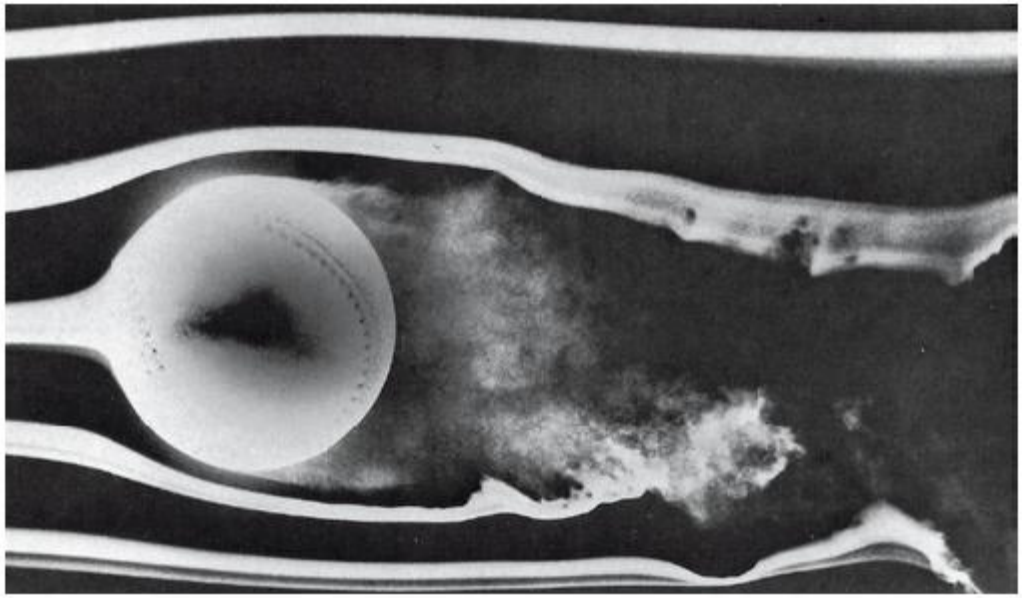

Figure 73. Smoke photograph of flow over a stationary (nonspinning) baseball. Flow is from left to right. Photograph by F.N.M. Brown, University of Notre Dame (Brown 1971, Mehta 1985).

Some results

- The spin produces the Magnus force that makes it curve downward, faster than it would under the action of gravity alone.
- The influence of Gravity is comparatively pronounced at the end of trajectory.
- The seam produces an overall roughness that helps to reduce the critical Reynolds number, indicating early transition to transcritical region. Seam orientation plays an essential role. e.g. 2 seam has a much higher C_L than 4-seam at low S, but collapse when S is above 0.4.
- C_L is mainly related to S (Spinning factor) and is a weak function of Reynolds number.
- Normally $S < 0.4$ for baseball.

The Knuckleball Baseball (Nonspinning)

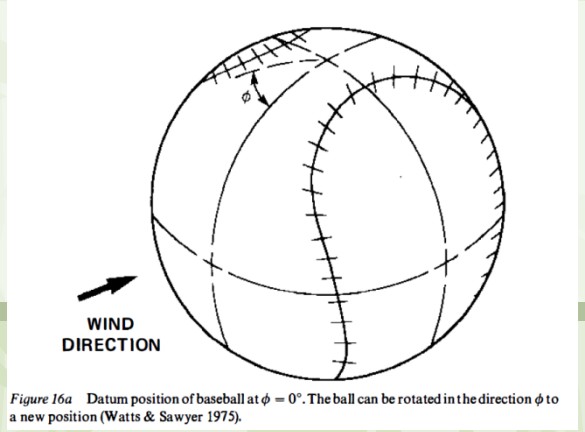

Figure 16a Datum position of baseball at $\phi = 0°$. The ball can be rotated in the direction ϕ to a new position (Watts & Sawyer 1975).

- At $\phi = 0^{\circ}$, the normalized lateral force (F/mg) was zero, but as the ball orientation was changed, values of F/mg = $\pm$0.3 were obtained with large fluctuations (F/mg~0.6) at $\phi = 50^{\circ}$. These large fluctuating forces were found to occur when the seam of the baseball coincided approximately with the point where boundary-layer separation occurs, an angle to the vertical of about 110°. The separation point was then observed to jump from the front to the back of the stitches and vice versa, thereby producing an unsteady flow field.

國立交通大學
National Chiao Tung University

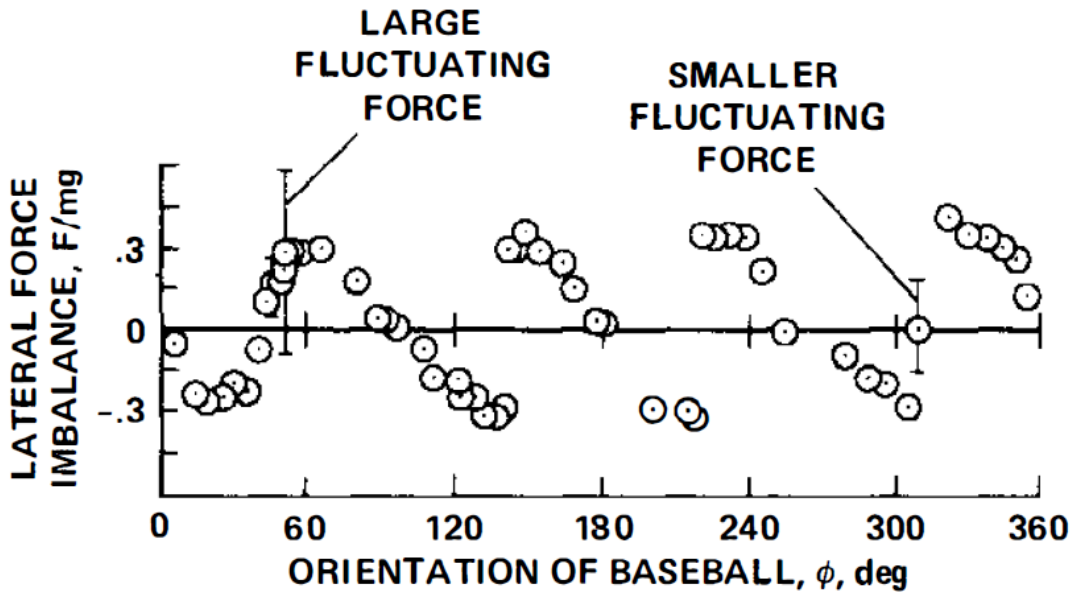

Figure 16b The variation of the lateral force imbalance with orientation of the baseball—see Figure 16*a* for definition of ϕ (Watts & Sawyer 1975).

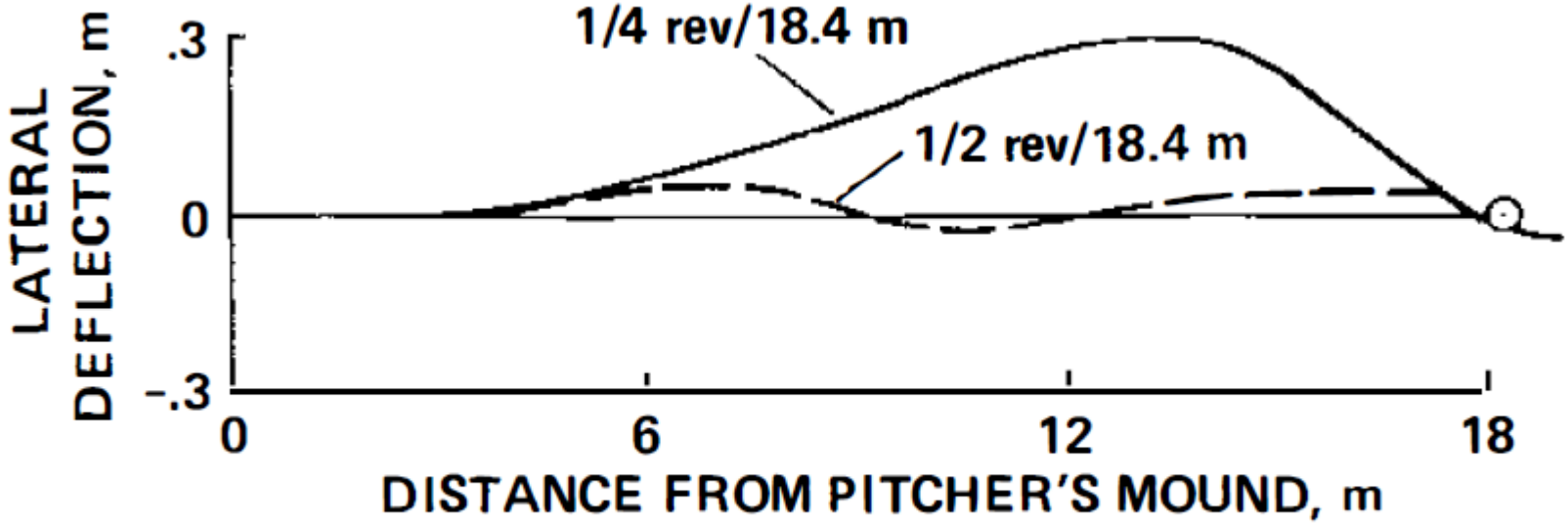

Figure 19 Typical computed trajectories for a slowly spinning baseball, with $U = 21$ m s^{-1} (Watts & Sawyer 1975).

- Watts & Sawyer (1975) suggest that erratic trajectory when the ball is so released that the seam lies close to the separation point.
- Weaver (1976) rightly points out, a baseball thrown with zero or near-zero spin will experience a torque due to the flow asymmetry that will cause the ball to rotate.

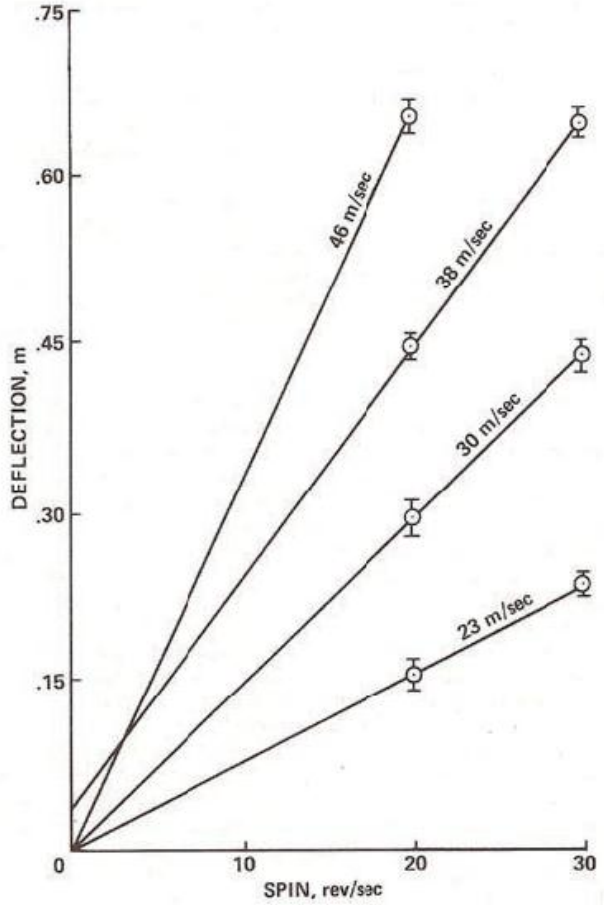

Figure 74. Lateral deflection of a baseball, spinning about a vertical axis, when dropped across a horizontal airstream. These values are for the same time interval (0.6 seconds), the time required for the ball to cross the airstream (Briggs 1959, Mehta 1985).

Golf Ball

- What is role of the dimples? (~380 dimples)
  - The major drag is pressure drag not skin drag.
  - The pressure drag is reduced when the boundary layer is turbulent and separation is delayed.
  - The variation of critical Reynolds number casts an momentous role
  - Re_{cr}: transition of laminar BL to turbulent BL

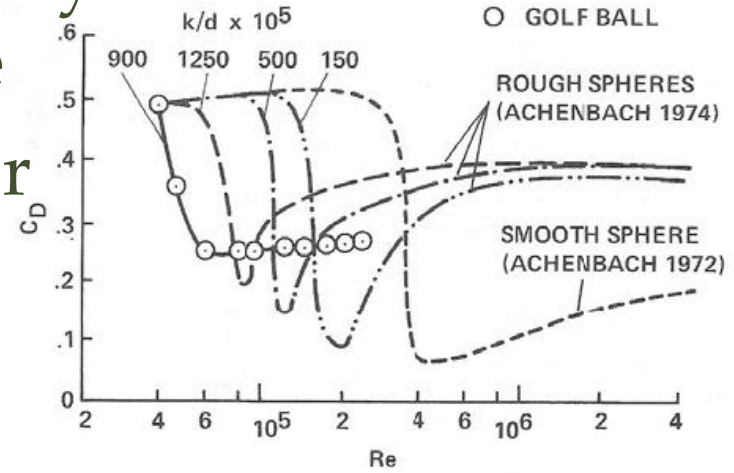

Figure 42. Variation of golf ball and sphere drag, where k is the sand-grain roughness height and d is the ball diameter (Bearman and Harvey 1976, Mehta 1985).

Golf Ball

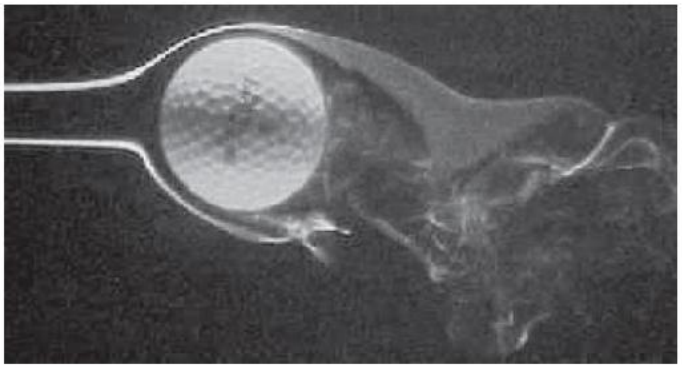

Figure 43. Flow visualization of a spinning golf ball at $Re = 1950$. Flow is from left to right and the ball is spinning in a clockwise direction at 0.5 revs/sec (Pallis and Mehta 2003).

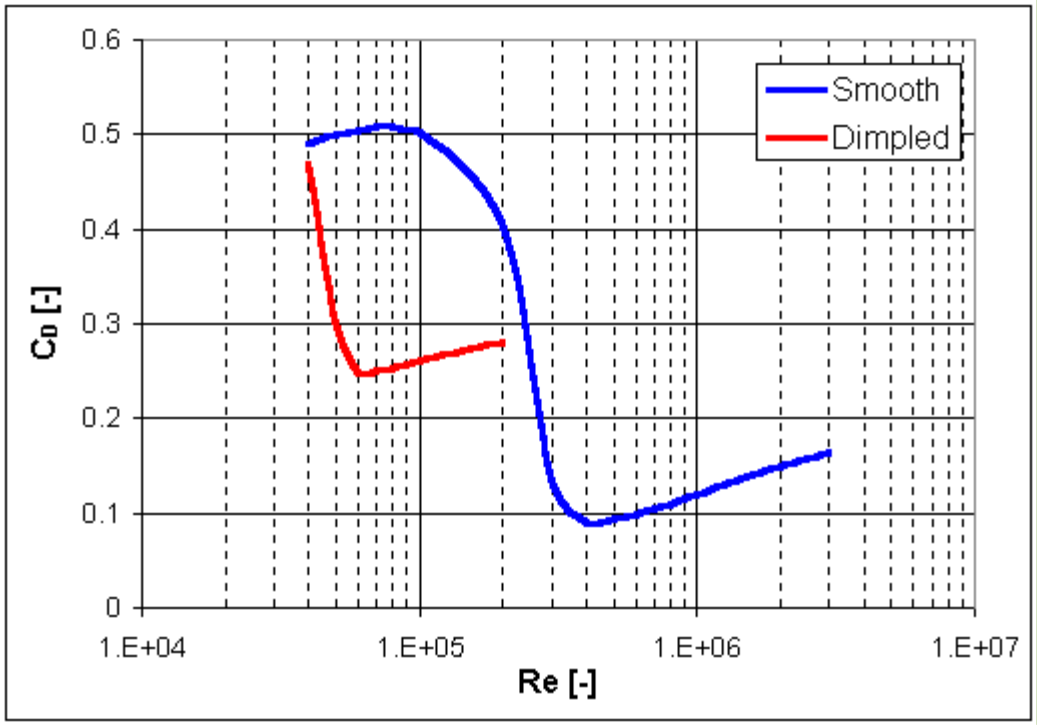

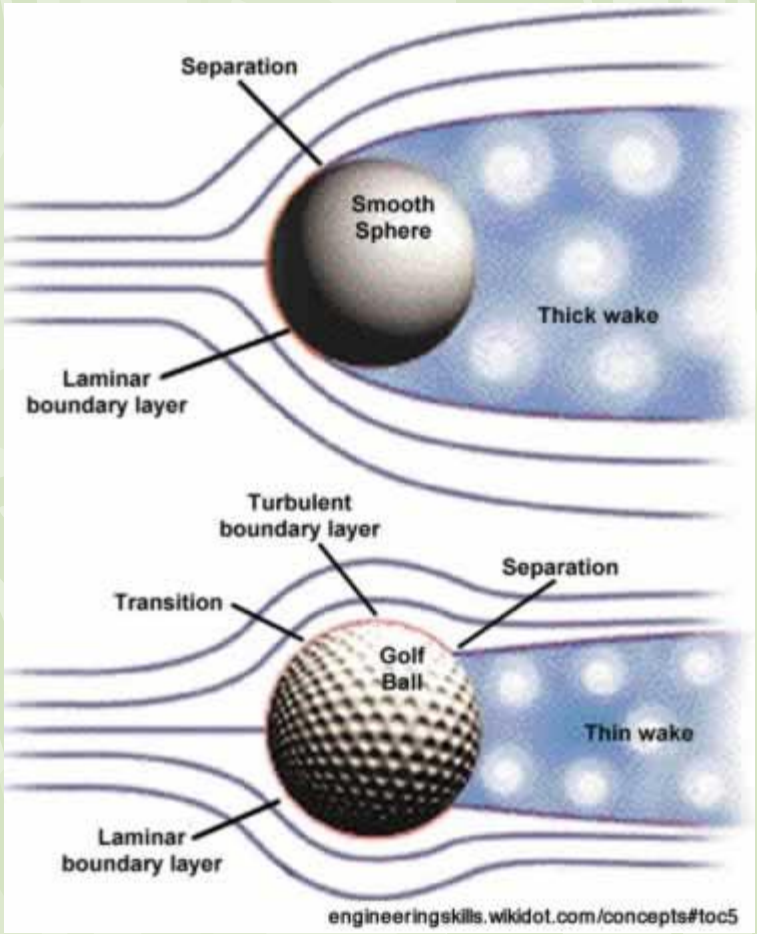

Influence of dimple configurations..

- Optimized dimple depth is around 0.25 mm.
- Bearman & Harvey (1976) concluded that hex-dimple is superior to conventional golf ball. (6 m longer range)

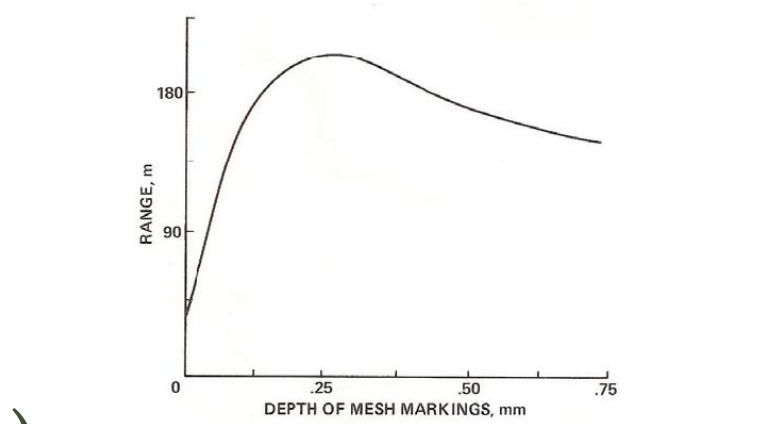

Figure 51. Effect of square dimple depth on range (Cochran and Stobbs 1968, Mehta 1985).

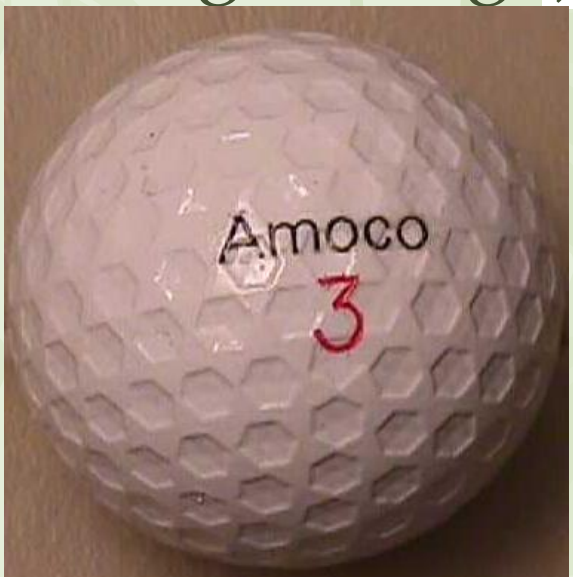

Influence of dimple configurations..

- Hex dimple shows lower form drag (about 6%).
- Possible due to shedding of longitudinal vortices caused by the sharp edge.

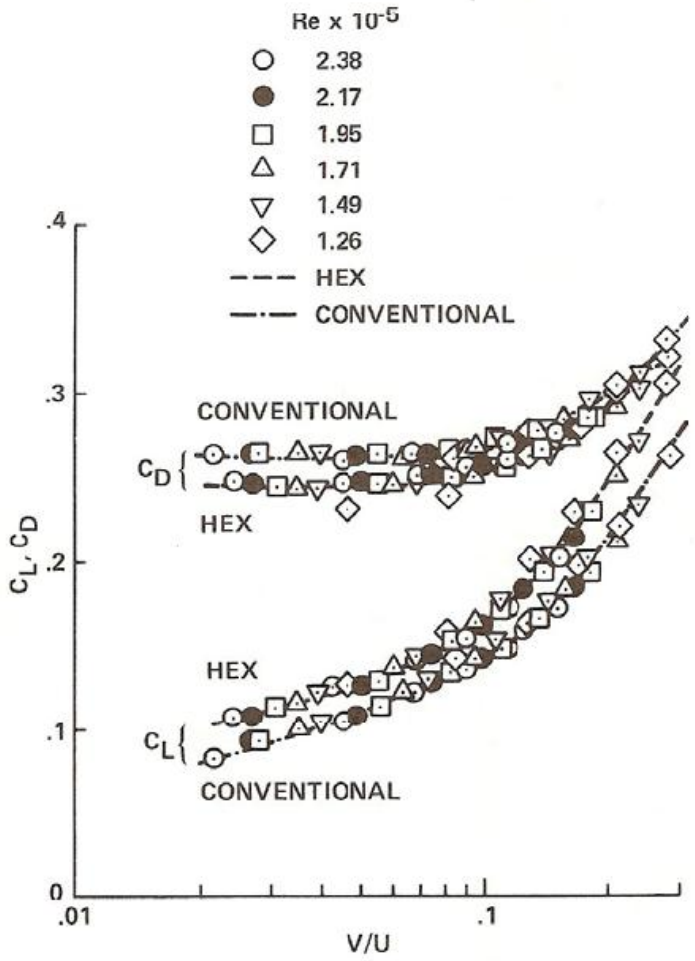

Figure 54. Comparison of conventional and hex-dimpled golf balls (Bearman and Harvey 1976, Mehta 1985).

Influence of dimple configurations..

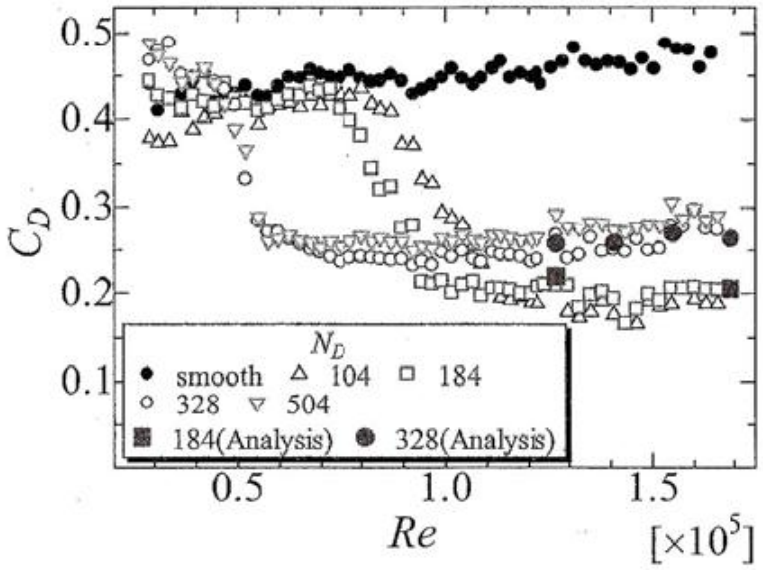

Figure 53. Variation of drag coefficient with Reynolds number: effects of number of dimples (Aoki et al. 2004).

Table 1 Specifications of spherical surface.

N_D	b [mm]	c [mm]	k [mm]
smooth	-	-	-
104	3.897	3.528	0.338
184	2.043		
328	0.650		
504	0.297	3.046	0.292

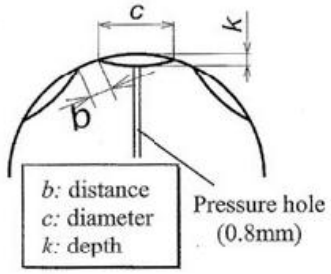

Figure 52. Details of dimple variations tested (Aoki et al. 2004).

Mechanism of Drag Reduction

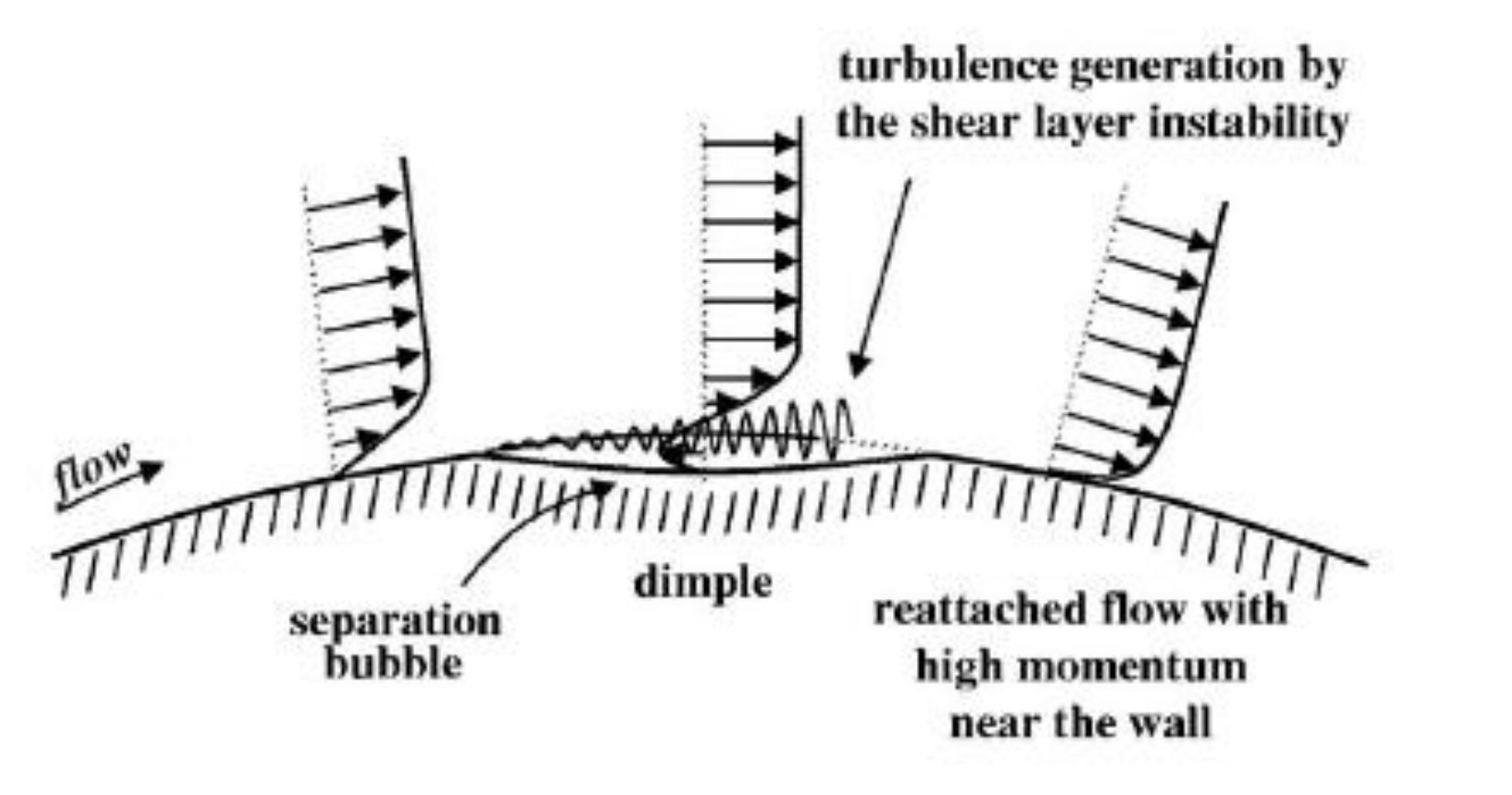

PHYSICS OF FLUIDS 18, 041702 (2006)

Mechanism of drag reduction by dimples on a sphere

Golf Ball

- Forces & Trajectory

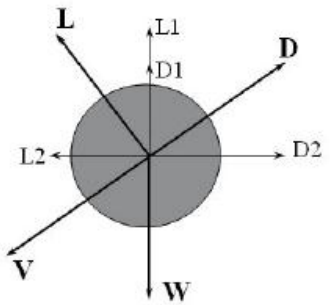

Descending Ball

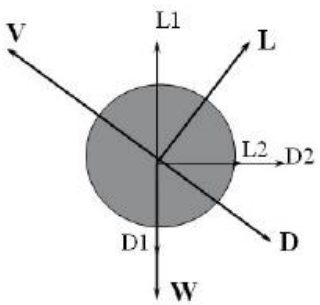

Ascending Ball

Figure 44. Schematic showing forces acting on a golf ball in flight for descending and ascending conditions (based on Smits and Ogg 2004a,b).

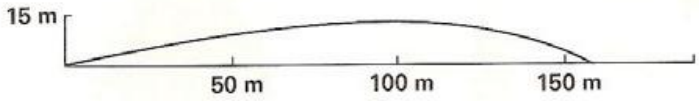

Figure 45. Typical golf ball trajectory. Initial conditions: velocity = 57.9 m/s, elevation = 10, spin = 3500 rpm (Bearman and Harvey 1976, Mehta 1985).

Estimated drag coefficient vs. Re Alaways (1978)

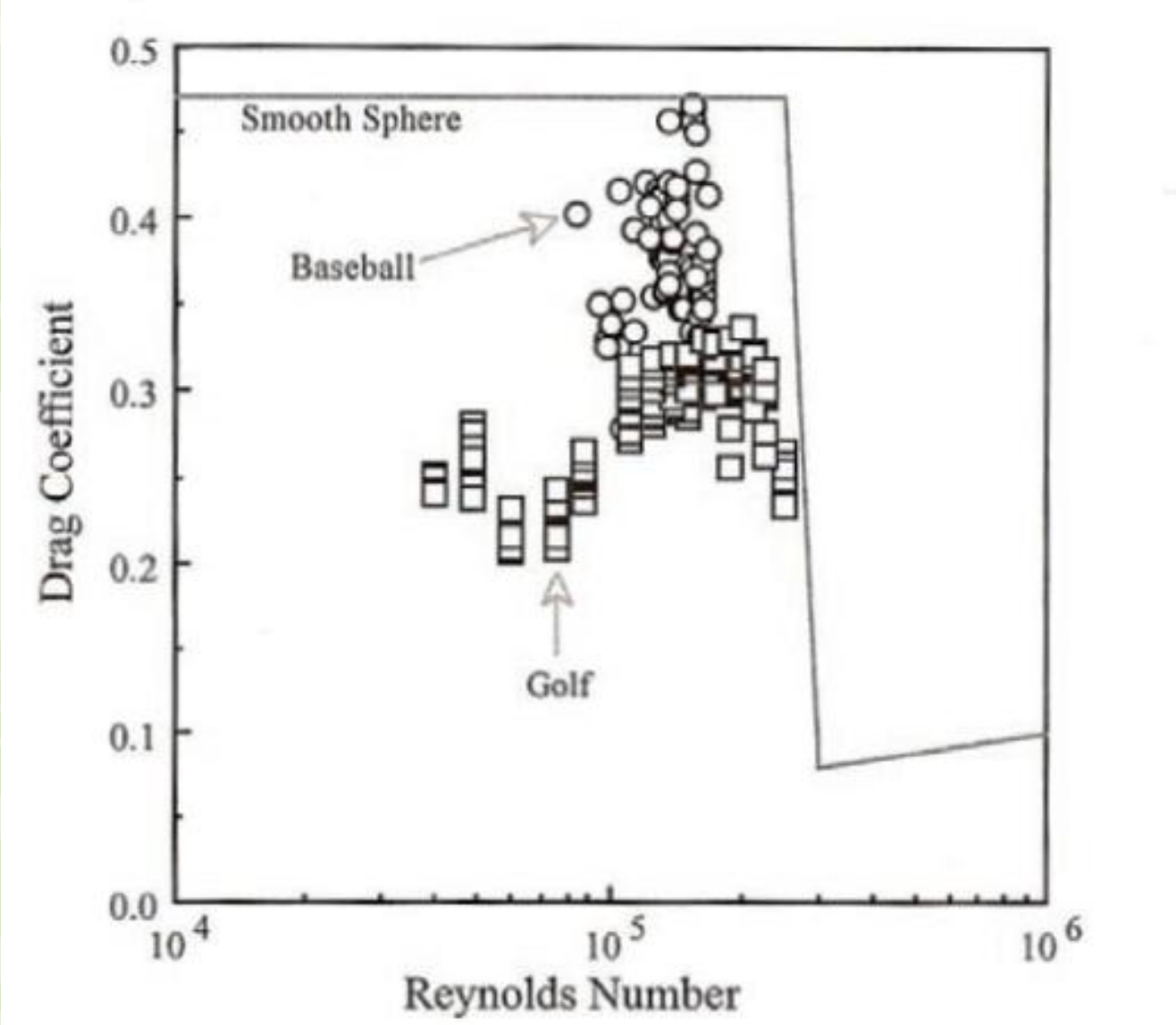

Tennis Ball

- Unlike the baseball, the non-spinning tennis ball did not show significant asymmetric BL. separation subject to change of seam orientation.

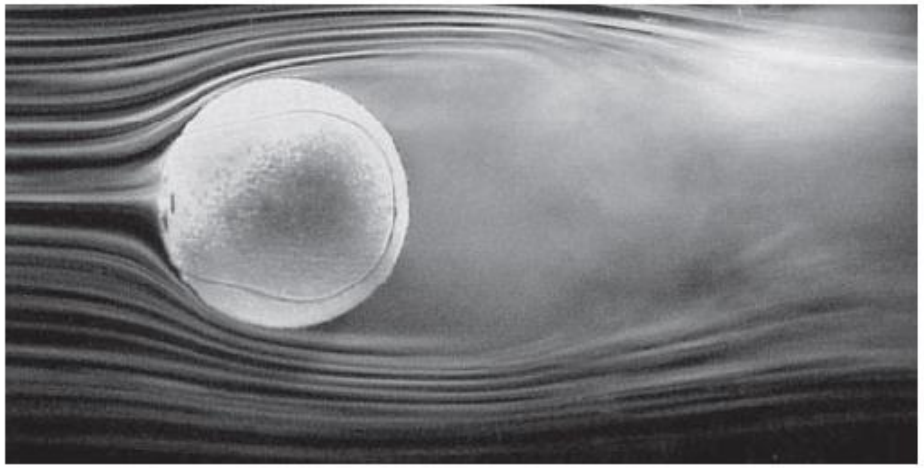

Figure 27. Flow visualization of 28 cm diameter tennis ball model with no spin (Re = 167,000). Flow is from left to right (Mehta and Pallis 2001b).

Tennis ball - spinning

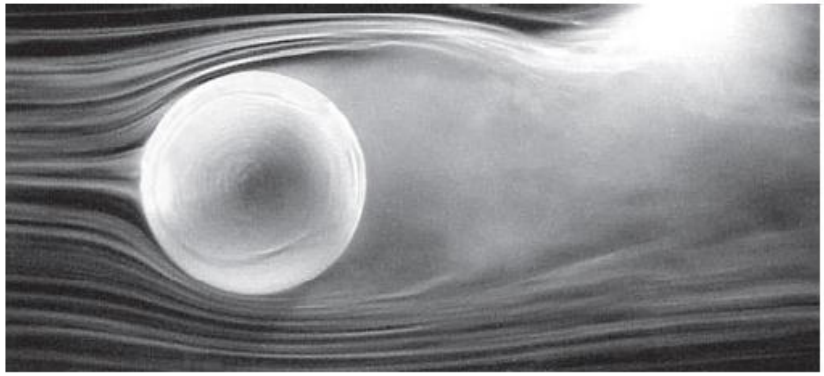

Figure 28. Flow visualization on ball with topspin (counter-clockwise rotation at 4 revs/sec, Re = 167,000). Flow is from left to right (Mehta and Pallis 2001b).

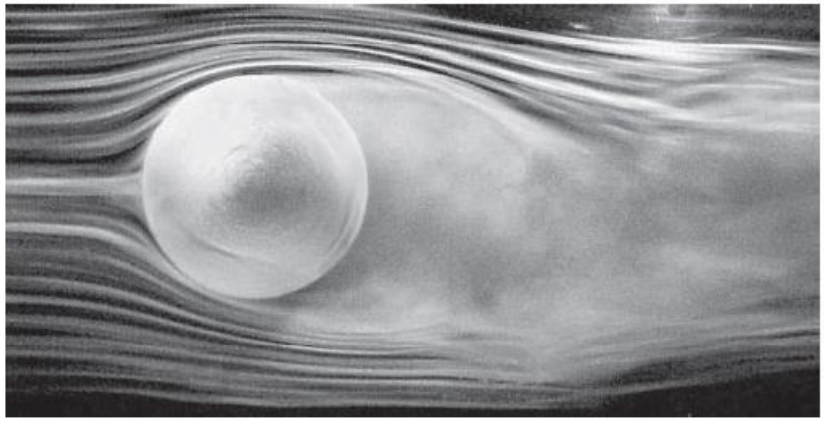

Figure 29. Flow visualization on ball with underspin (clockwise rotation at 4 revs/sec, Re = 167,000). Flow is from left to right (Mehta and Pallis 2001b).

- C_d is relatively high for a new tennis ball ~0.6~0.7.
- C_d is almost independent of Re, or slightly decreasing with Re, implying an early transition to supercritical regime.

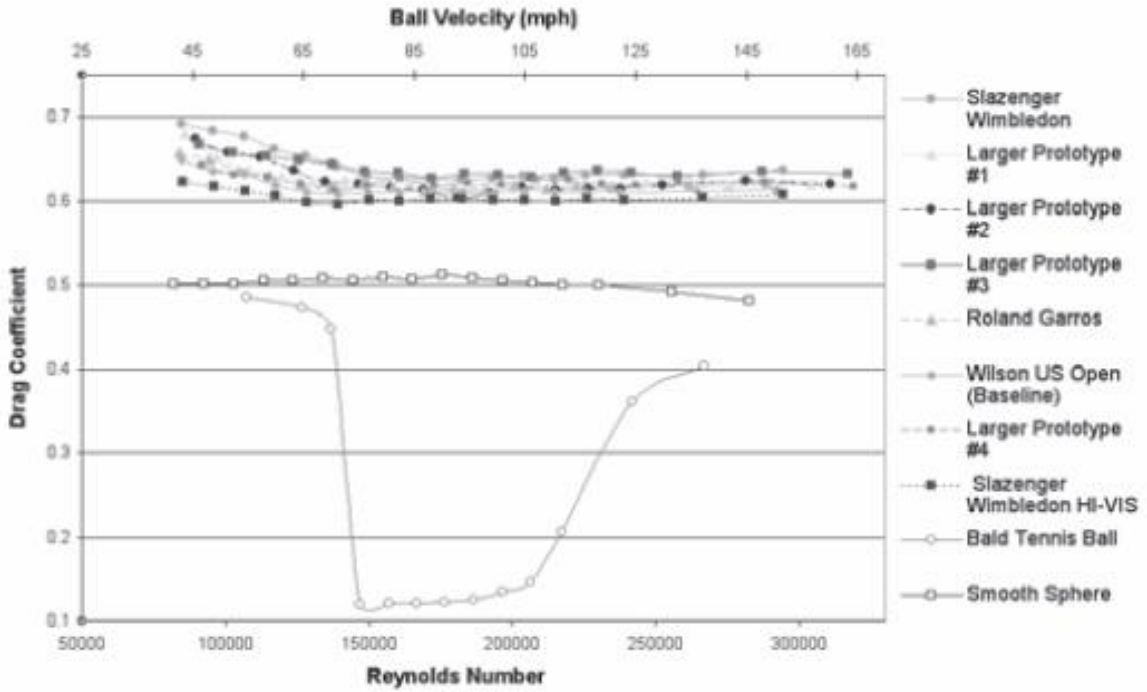

Figure 31. Drag Coefficient versus Reynolds Number for new tennis balls (Mehta and Pallis 2001b).

Influences of Impacts

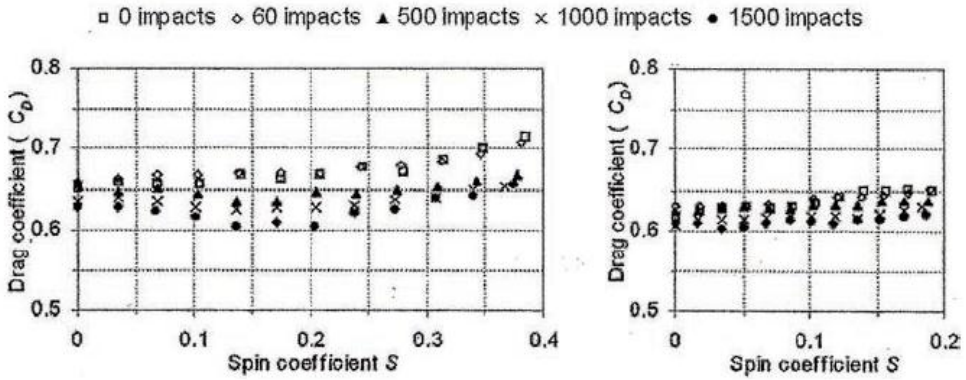

Figure 37. Drag Coefficient for spinning balls. (a) $U = 25$ m/s (Re= 105,000); (b) $U = 50$ m/s (Re=210,000) (Goodwill and Haake 2004).

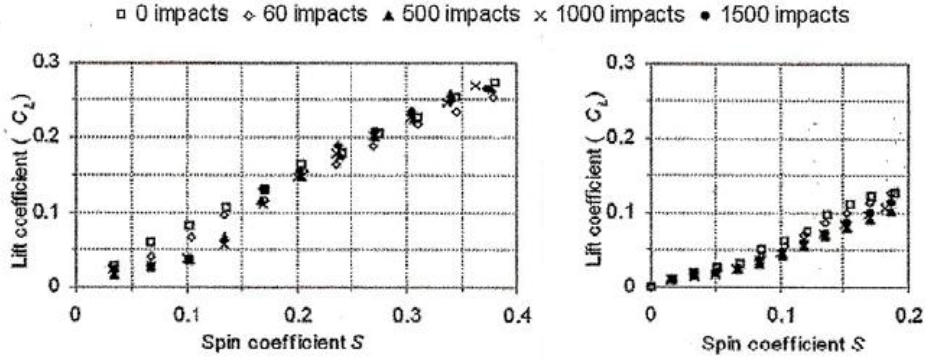

Figure 38. Lift Coefficient for spinning balls. (a) $U = 25$ m/s (Re= 105,000); (b) $U = 50$ m/s (Re=210,000) (Goodwill and Haake 2004).

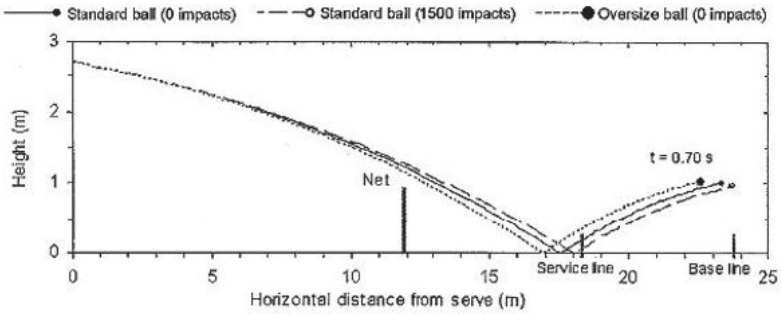

Figure 39. Predicted trajectory for new and worn standard size balls and an oversize ball (Goodwill and Haake 2004).

- Drag coefficient changes..

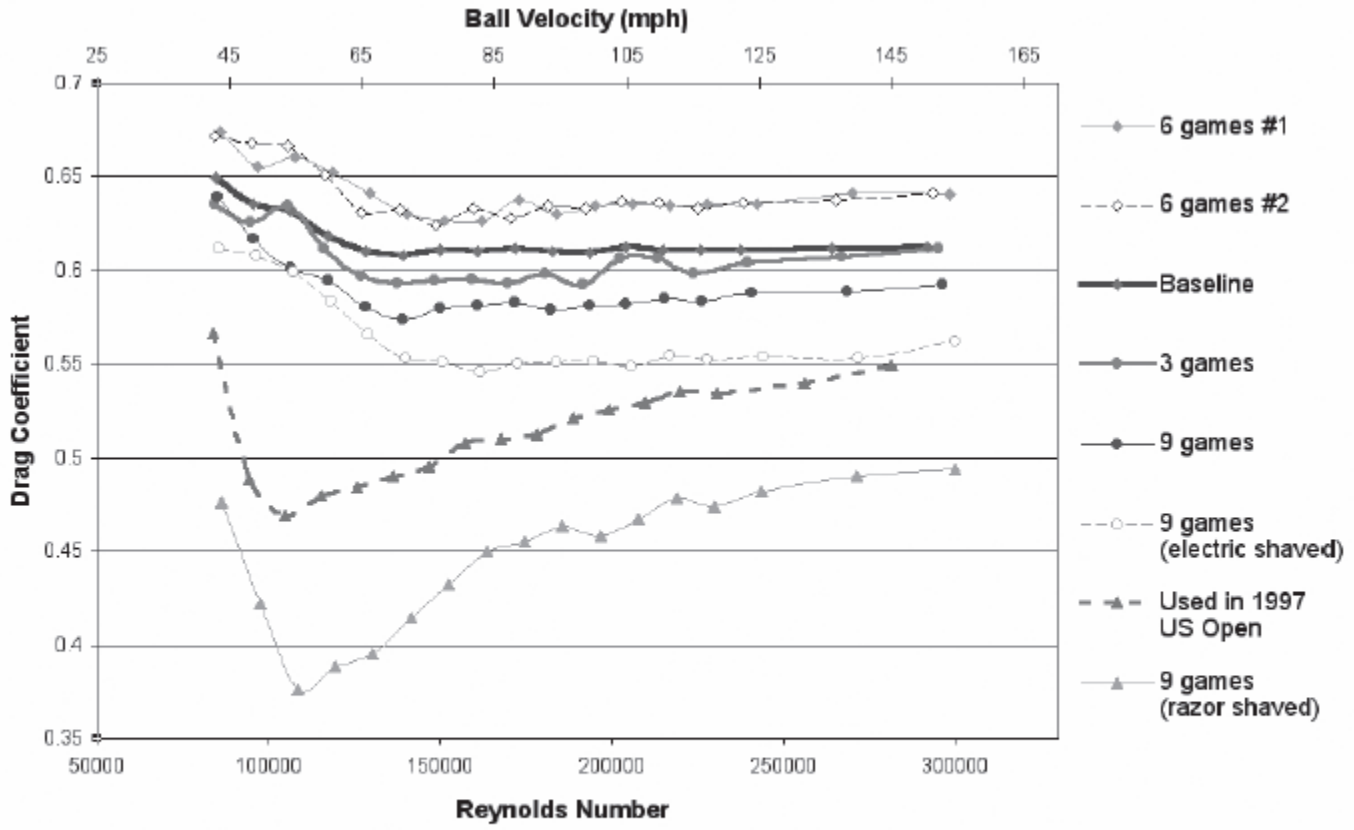

Figure 35. Drag Coefficient versus Reynolds Number for used Wilson US Open balls (Mehta and Pallis 2001b).

Table Tennis (40 mm, 2.7g)

- Objective:
  - Visual observations of the trajectory of the table tennis ball

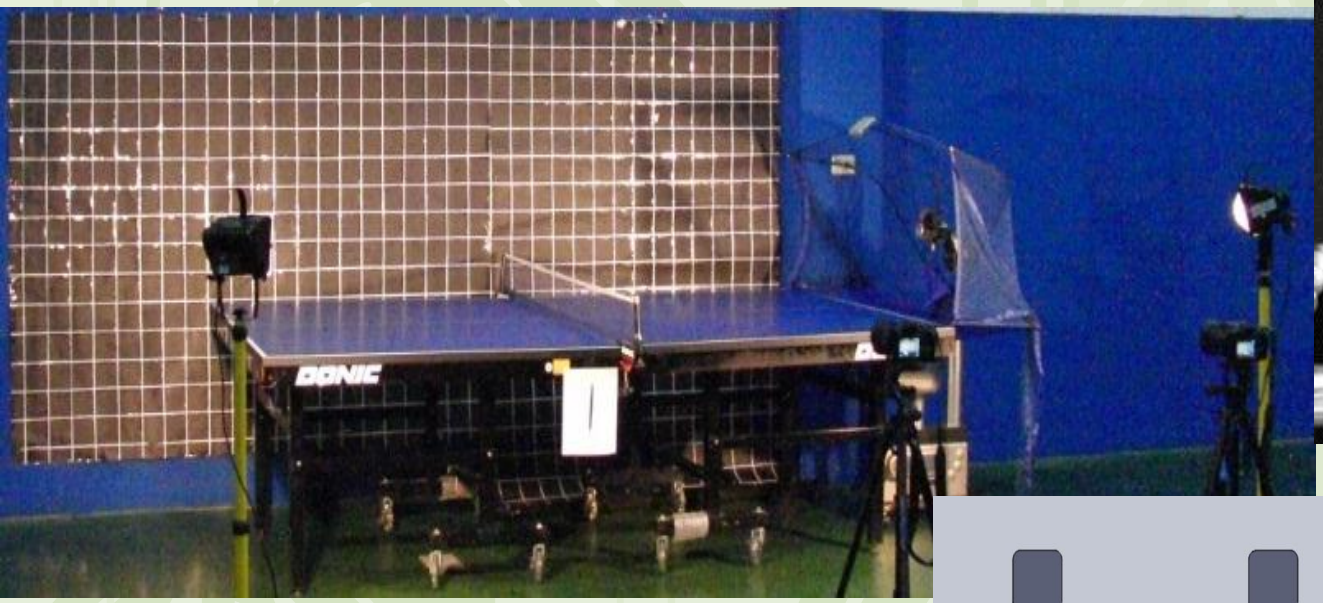

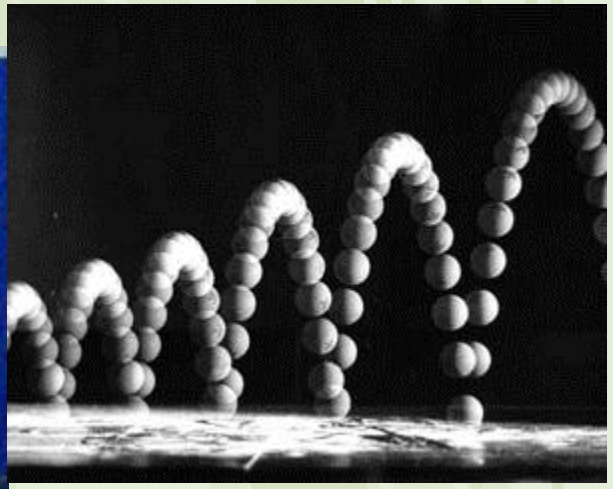

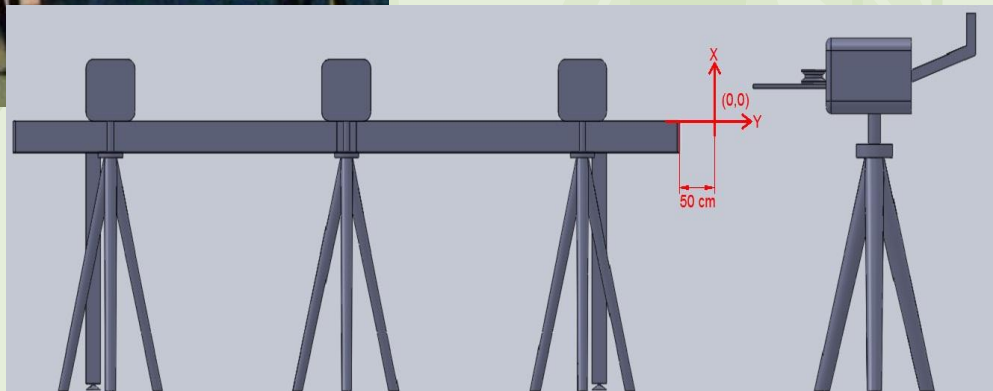

Descending acceleration and the angular velocity of the flying table tennis ball subject to initial velocity.

		a_y (m/s^2)	
	Initial	On Net	Leaving table
Low Speed V_i = 11.5 m/s	-22.6	-21.86	-22.29
High Speed V_i = 15.7 m/s	-24.6	-22.13	-23.89
		ω (r/s)	
	Initial	On Net	Leaving table
Low Speed V_i = 11.5 m/s	68.33	56.67	29.61
High Speed V_i = 15.7 m/s	87.03	85.5	59.44

Trajectory of the topspin ball subject to initial velocity and their comparisons against frictionless and irrotational ball

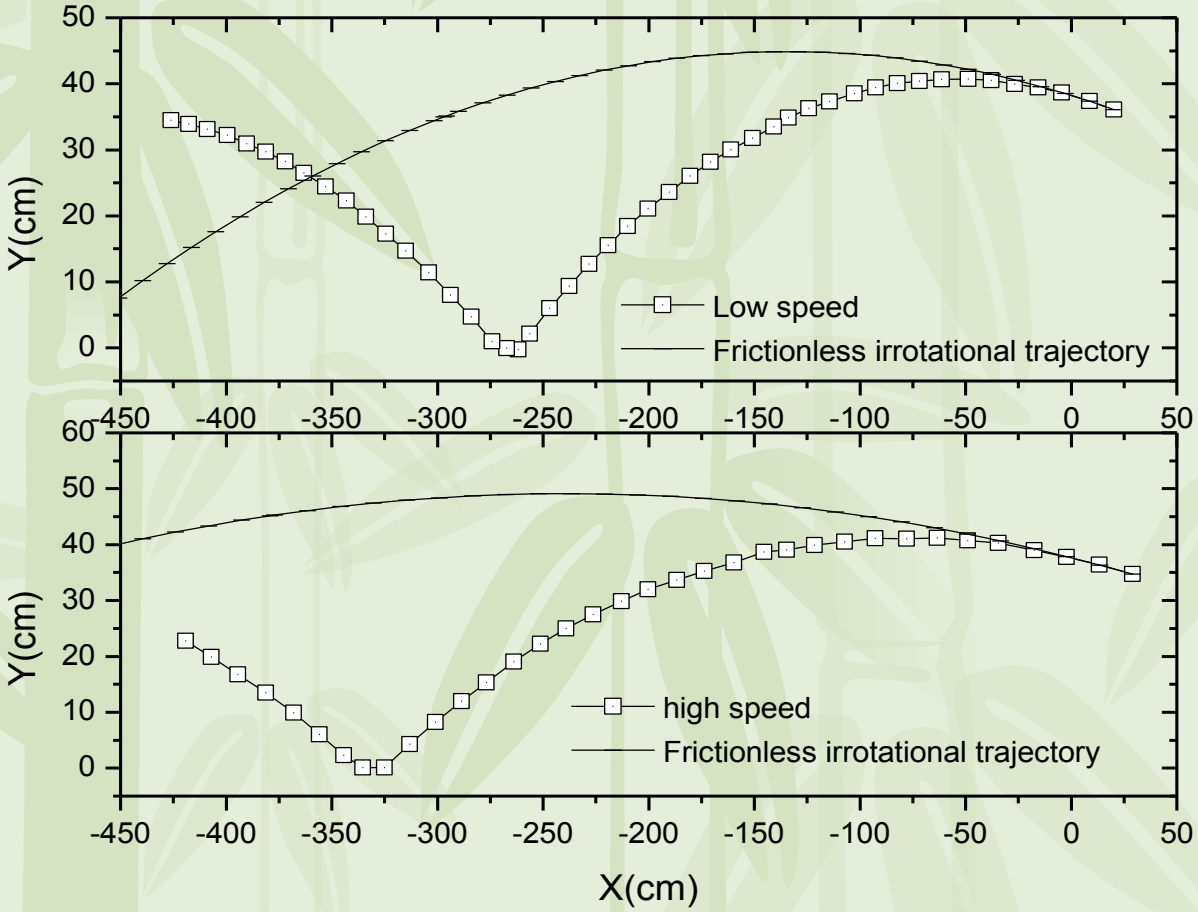

Observations..

- The observed trajectory shows significant departures to the frictionless, irrotational ball due to Magnus force and imposed drag.
- The initial velocity casts an influence of V_x whereas the effect on V_y is quite small.
- A significant velocity surge appears right just impact for either V_x or V_y, the formal surge phenomenon appears due to the nature of topspin ball where the latter is subject to significant reaction force. The surge phenomenon becomes more pronounced with the rise of initial velocity.

Observations..

- Normally the angular velocity decreases slightly along the flight line, the deterioration is more severe when the initial velocity is low. However, a significant reduction of angular velocity is observed after impact, this is applicable for either low or high initial velocity. However, higher initial velocity will retain more its angular velocity after impact.

Measured V_x and V_y subject to initial velocity (a) V_x; and (b) V_y

(a) V_x

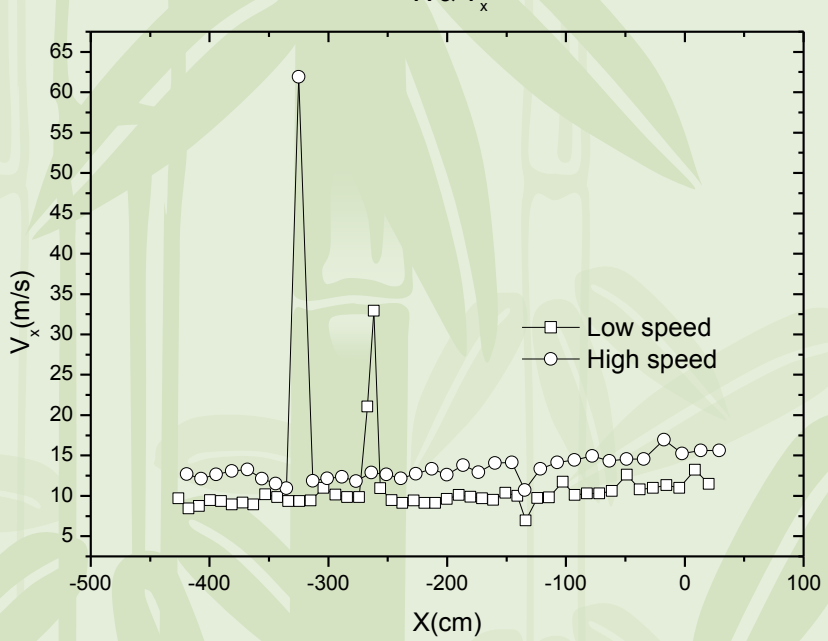

(b) V_y

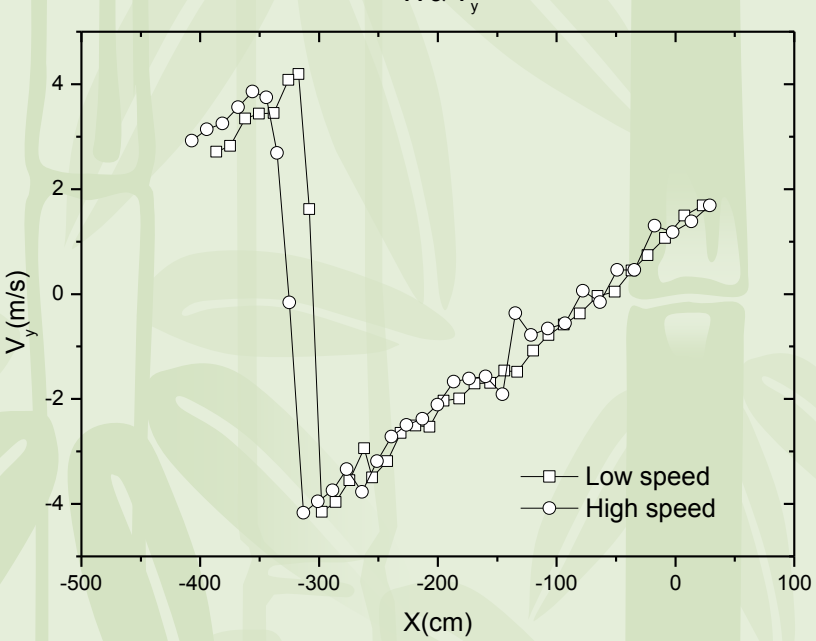

Summary

- Aerodynamics plays an essential role in sports ball.
- The presence of spinning significantly alters the trajectory of the sports ball.
- Surface condition also cast a pronounced influence on the aerodynamics of sports ball. For instance, roughness, fuzz, dimple, seam, and the like.

Some researches deserve going further

- Impact – with and without spinning, normal impact and oblique impact.
  - Change significantly with the sport ball.
- Impact – Influence of the contact surface.
- Lift, Drag, Magnus force pertaining to the initial tossing – variation of the sports ball from supercritical, critical to subcritical region.

General References

- R.D. Mehta, "AERODYNAMICS OF SPORTS BALLS," Ann. Rev. Fluid Mech. 1985. 17: 151-89.
- R.D. Mehta, "SPORTS BALLS AERODYNAMICS," in SPORT AERODYNAMICS, pp. 229-331. edited by H. NØRSTRUD, Springer 2008.
- C.E. Smith et al., "Numerical investigation of the flow over a golf ball in the subcritical and supercritical regimes," Int. J. Heat and Fluid Flow. 2010. 31:262–273

Acknowledgements

Supporting fund from the diamond project of the National Chiao Tung University and some technical assistance from the arena sports group.

Peoples who assist the on-going project:

Feng-Yun Yu[1]
[1]Office of Physical Education

Po-Lung Tien[2]
[2]Department of Electrical Engineering,

Hsien-Kuo Chang[3]
[3]Department of Civil Engineering,

Sien Chi[4],
[3]Department of Photonics Engineering,

Huai Po Lo[4]
[4]Department of Mechanical Engineering,

Aerodynamics of the Curve-Ball: An Investigation of the Effects of Angular Velocity on Baseball Trajectories

By

LEROY WARD ALAWAYS
B.S. (California State University, Chico) 1984
M.S. (University of California, Davis) 1987

DISSERTATION

Submitted in partial satisfaction of the requirements for the degree of

DOCTOR OF PHILOSOPHY

in

Engineering

in the

OFFICE OF GRADUATE STUDIES

of the

UNIVERSITY OF CALIFORNIA

DAVIS

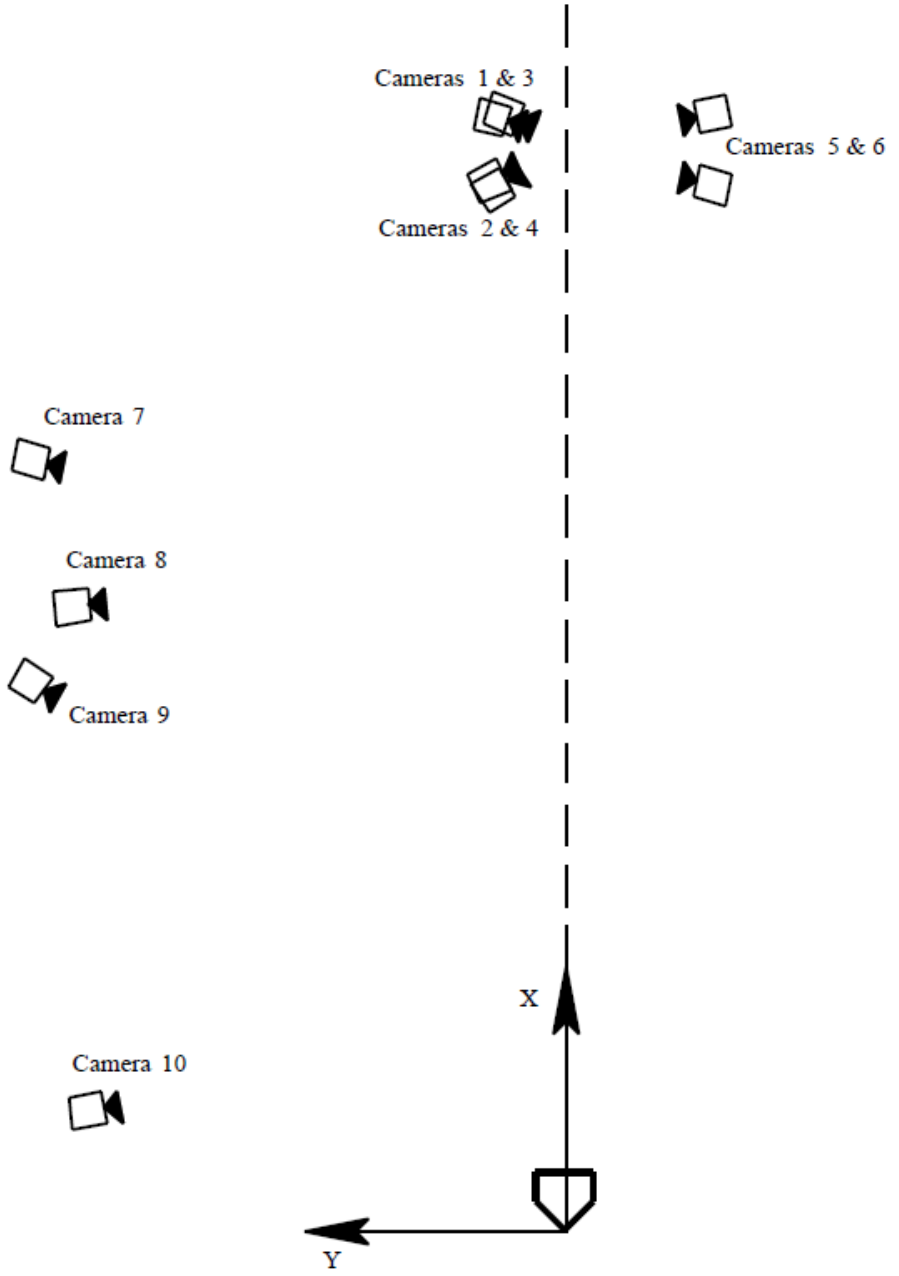

Figure 3–3: Top view of camera layout for the pitcher trials.